Enhanced annealing of the dislocation network under irradiation

Dan Mordehai
Department of Materials Engineering, Technion - Israel Institute of Technology, 32000 Haifa, Israel

Georges Martin
CEA-Siège, CAB. H.C., 91191 Gif-sur-Yvette Cedex, France

(Received 22 March 2011; revised manuscript received 9 May 2011; published 28 July 2011)

In crystalline metals, the dislocation network is the main source of internal strain, while irradiation steadily injects new sources of internal strain (point defects, defect clusters). As a consequence, the evolution of the dislocation network is driven by irradiation. While the atomistic mechanisms by which the forcing proceeds have long been suggested, namely the partitioning of defect elimination between dislocations and other defect sinks, both in stationary or transient regimes, some of the macroscopic consequences, such as irradiation enhanced dislocation annealing and irradiation driven recrystallization, are left unexplained. In this work we show that dislocation sink strengths for point defects are altered in the presence of neighboring dislocations and their climb motion is coordinated with the dislocation microstructure. A climb model, which takes into account the dislocation network, provides the mechanism for coordinated climb, which is shown to ease dislocation annealing. In particular, we demonstrate that coordinated dislocation climb accelerates the annihilation of dislocation pairs with the opposite sign and the repulsion of dislocations of the same sign, thereby, among other things, promoting the annealing of small-angle tilt boundaries by subgrain rotation.

DOI: 10.1103/PhysRevB.84.014115 PACS number(s): 61.82.Bg, 61.72.jd, 61.72.jj, 61.72.Lk

I. INTRODUCTION

The evolution of the microstructure of metals under irradiation is a complex process, with still unexplored and poorly understood areas. Point defects (vacancies and self-interstitial atoms) are produced by the nuclear collisions, at a rate proportional to the irradiation flux (or dose rate); therefore their concentration in the bulk deviates from the thermal equilibrium value. Because of point defect jumping from lattice site to lattice site, several annealing processes occur, such as vacancy-interstitial mutual recombination, point defect elimination on lattice discontinuities (dislocations, grain boundaries, etc.) and point defect condensation into defect clusters (dislocation loops, stacking fault tetrahedrons, voids, etc.).[1] Defect jump is a thermally activated process, hence the rate of the recovery processes depends on temperature; beyond some critical irradiation dose, the elimination processes compensate the production of defects; the defect concentrations achieve a value which, for given temperature and dose rate, depends on the slowly varying microstructure (as defined by the density and geometry of sinks). The evolution of the microstructure under irradiation is thus determined by the net current of defects to the various defect sinks it is made of. The current of interstitials (or vacancies) to a given sink is made of two contributions: random walk and drift by the force, which results from the physical interaction of the defect with the sink structure [see Eq. (1) below].[2] In the present work, we focus on the elastic interaction between the defects and the local strain field.

Experimental observations reveal an intriguing phenomenon. At intermediate temperatures, the dislocation density reaches a saturation value, which is independent of the inherited population from the initial thermomechanical treatment.[3] Northwood found that the microstructure of annealed and cold-worked zirconium-based alloys was indistinguishable after irradiation at 300 °C.[4] Similar results were reported by Maziasz in austenitic steels up to a temperature of 440 °C.[5] Indeed, it is documented that the pre-existing network disappears after a few displacements per atom and is replaced by a population of interstitial loops, which eventually grow into a new dislocation network, independently of the initial network.[5,6] The recovery of the initial dislocation network was observed also by Vardiman in aluminum.[7] It is sometimes argued that the so-called high burnup structure in uranium dioxide and in fuel pellets (HBS: the occurrence of grain refinement in heavily irradiated zones) results from annealing of the dislocation network.[8] It is clear that thermal recovery is insufficient to elucidate these observations and one should consider the possibility of an irradiation-induced recovery of the inherited dislocation network. In this work, we provide a clarification of the following question: by which process might irradiation promote or enhance the recovery of the initial dislocation network?

Modeling the development of the microstructure in materials under irradiation deals with the long-term evolution of the dislocation network. For edge dislocations to anneal, two processes must operate: climb must be active for dislocations to overcome obstacles (and allow glide toward dislocation with opposite sign) and the climb of neighboring dislocations must be coordinated in such a way that dislocations with opposite sign will merge while dislocations with the same sign will escape one another. Wolfer[9] proposed a simple phenomenological model, where the dislocation density evolves as a balance between multiplication and annihilation. Valentin and Martin modeled the evolutions of various types of defect clusters together with the climb of the dislocation network.[10] Later, Wolfer and Glasgow shed light on the physical coefficients of the phenomenological multiplication-annihilation model.[11] However, the interstitial flux in this work was independent of the dislocation network. Moreover, the irradiation contribution in all models of dislocation climb is insensitive to the dislocation network. In that sense, the climb model considered by

Wolfer and Glasgow, and by many others (e.g., Refs. 12–14), elucidates the irradiation enhanced annihilation rate of edge dislocations of opposite sign separated by a vacancy-type ribbon [e.g., Fig. 1(b)], but implies slowing down in the case of an interstitial-type ribbon [e.g., Fig. 1(a)]; similarly, the latter model predicts no alteration under irradiation of the effective repulsion among dislocation of the same sign, hence no specific mechanism for sub-boundary annealing. A proper treatment of how dislocations climb under irradiation in the presence of a dislocation network is thus of interest and is still lacking, to our knowledge.

We show in this work that taking into account the presence of the dislocation network when calculating the climb rate of one specific dislocation under irradiation points to new irradiation enhanced annealing mechanisms of the dislocation network. After briefly reviewing in Sec. II the models describing the climb rate of an isolated dislocation under irradiation, without accounting for neighboring dislocations, we present in Sec. III a general treatment to calculate flux of point defects to a dislocation, in the presence of a dislocation microstructure. We then illustrate the model on a few simple dislocation structures: dislocation pairs (Sec. IV), dislocation dipoles (Sec. V), and on the evolution of the misorientation of a low-angle tilt boundary (Sec. VI).

II. CLIMB OF ISOLATED DISLOCATIONS

A. Sink strength of isolated dislocations

Classical models assume that dislocation climb is controlled by the diffusion of point defects (vacancies and interstitials independently) to or away from the dislocation. The flux of point defects in the bulk is determined by the gradient of their respective chemical potential $\mu(\mathbf{r})$ in the matrix

$$\mathbf{J} = -\frac{Dc}{kT}\nabla\mu = -D\nabla c - Dc\nabla\psi, \tag{1}$$

where $c(\mathbf{r})$ is the point defects concentration (either vacancies or interstitials), D is the diffusion coefficient of point defects, and $kT\psi(\mathbf{r})$ is the interaction energy of a point defect with the matrix (kT has its usual meaning). We recognize in Eq. (1) the two contributions we discussed in the Introduction: random walk and drift, which respectively translate into a diffusive and a convective flux. The latter is strongly dependent on the local strain field, i.e., the climb rate depends on the spatial distribution of the strain within the bulk. At this stage of our discussion it is sufficient to assume that all interaction energies in this work are harmonic ($\triangle\psi = 0$). Then, the steady-state concentration of point defects satisfies

$$\triangle c + \nabla c \cdot \nabla\psi = 0. \tag{2}$$

We consider the dislocation to be an isolated sink of radius r_d, with an imposed equilibrium concentration of point defects c_d in its vicinity. Far from the dislocation, at a distance denoted as r_∞, the point defects concentration is hypothesized to be uniform c_∞. Under nonirradiating conditions in a defect-free crystal this concentration has its thermal equilibrium value c_0. Irradiation increases the concentration of point defects above the thermal equilibrium value ($c_\infty > c_0$) and a diffusion flux results toward the sinks [first term in the right-hand side of Eq. (1)]. The climb rate is obtained from the net flux of point defects (either vacancies or interstitials) from and into the dislocation core and has the form

$$v_{cl} = \frac{\Omega}{b} Z D\,(c_\infty - c_d)\,, \tag{3}$$

where b is the Burgers vector, Ω is the atomic volume, and Z is a dimensionless geometric factor, known as the sink strength, which is a means to quantify the dislocation capacity to absorb or emit point defects from or into the bulk.

In the case of vacancies, the interaction energy between vacancies and the climbing dislocation is usually omitted ($\psi = 0$), because it is small compared to that of interstitials. Thus the solution of Eq. (2) yields a sink strength for vacancies, independent of the material:[15]

$$Z_v = \frac{2\pi}{\ln(r_\infty/r_d)}. \tag{4}$$

On the other hand, because of the strong polarizability of dumbbell interstitials, the interaction energy of the latter with a dislocation strain field cannot be omitted when calculating the sink strength for interstitials. The interaction energy is calculated by considering the point defect as an elastic inclusion within a strained medium.[16] An elastic inclusion can be characterized by the dipole tensor P_{ij}, which arises from the dilatation strain, and from its strain derivatives—the elastic polarizability tensor α_{ijkl}.[17,18] The latter terms arise from the difference in the elastic properties between those of the inclusion and those of the matrix. If one considers the elastic properties of the inclusion and the medium to be isotropic (with bulk modulus K^*, shear modulus G^*, and a pure dilatation strain ϵ^* for the inclusion and, respectively, K and G for the bulk), the interaction energy is[19]

$$\psi(\mathbf{r}) = \frac{1}{kT}[-K\Omega\mathrm{tr}(\epsilon_{ij})\epsilon^{\mathrm{misfit}} + \alpha^K \mathrm{tr}(\epsilon_{ij})^2 + \alpha^G \epsilon'_{ij}\epsilon'_{ij}], \tag{5}$$

where

$$\begin{aligned}
\epsilon^{\mathrm{misfit}} &= \epsilon^* \frac{3(1-\nu)K^*}{(1+\nu)K^* + 2(1-2\nu)K}, \\
\alpha^K &= -K\Omega \frac{3(1-\nu)(K-K^*)}{(1+\nu)K^* + 2(1-2\nu)K}, \\
\alpha^G &= -G\Omega \frac{15(1-\nu)(G-G^*)}{2(4-5\nu)G^* + (7-5\nu)G}.
\end{aligned} \tag{6}$$

ν is Poisson's ratio and $\epsilon'_{ij}(\mathbf{r})$ is deviatoric strain tensor,

$$\epsilon'_{ij} = \epsilon_{ij} - \tfrac{1}{3}\delta_{ij}\mathrm{tr}(\epsilon_{ij}). \tag{7}$$

The first term on the right-hand side of Eq. (5) arises from the interaction of the dilatation center with the medium whereas the second and third terms result from the inhomogeneity of the elastic properties of the interstitial in the matrix.

In the case of an isolated edge dislocation, the strain in the medium is the strain field induced by that dislocation. Employing the isotropic elasticity theory of dislocations, we

find that the interaction energy between an edge dislocation and a point defect is[19]

$$\psi(\mathbf{r}) = R_0 \frac{\sin\theta}{r} + O(r^{-2}), \tag{8}$$

where R_0 satisfies

$$R_0 = \frac{b}{2\pi} \frac{1-2\nu}{1-\nu} \frac{K\Omega\epsilon^{\text{misfit}}}{kT}. \tag{9}$$

$R_0/2$ is a typical length for the interaction, known also as the capture radius.[20] We notice that in this case only the size effect of the dilatation center gives rise to the main contribution, while the contribution of the inhomogeneity in the elastic constants (the interstitial polarizability tensor) results in short-range interactions of the order of r^{-2}.

Margvelashvili and Saralidze[21] solved Eq. (2), employing the interaction energy in Eq. (8), and found it to be of the form of Eq. (3) with a sink strength for interstitials

$$Z_{i,R_0} = 2\pi \frac{I_0(R_0/2r_d)}{I_0(R_0/2r_d)K_0(R_0/2r_\infty) - I_0(R_0/2r_\infty)K_0(R_0/2r_d)}, \tag{10}$$

where I_0 and K_0 are the modified Bessel functions of zero order. In the case of a strong interaction ($R_0 \gg r_d$), the sink strength is approximated,

$$Z_{i,R_0} \approx \frac{2\pi}{\ln(2r_\infty/R_0)}. \tag{11}$$

This result provides means to interpret the capture radius. Interstitials that enter the capture radius will be attracted to the dislocation and eliminate on its core. Thus the larger the capture radius (stronger interaction), the larger is the sink strength.

B. Climb rate

Interstitial and vacancy capture at the dislocation drive climb in opposite directions. For computing each defect flux to the dislocation, it is commonly assumed that within the distance r_∞, the vacancies and interstitials do not recombine. Thus the climb rate of a dislocation is the algebraic sum of the contribution from each type of point defects:

$$v_{cl} = \frac{\Omega_v}{b} Z_v D_v (c_{\infty,v} - c_{d,v}) - \frac{\Omega_i}{b} Z_i D_i c_{\infty,i}, \tag{12}$$

where $c_{d,v}$ is the equilibrium concentration of vacancies in the vicinity of the dislocation core. The thermal equilibrium concentration of self-interstitials is known to be zero in metals. In order to distinguish the contribution of irradiation to dislocation climb, the climb rate is written as the sum of two contributions: thermal climb (which is the climb rate in the absence of irradiation) and irradiation climb,

$$\begin{aligned} v_{cl,\text{therm}} &= \frac{\Omega_v}{b} Z_v D_v (c_{0,v} - c_{d,v}), \\ v_{cl,\text{irrad}} &= \frac{\Omega_v}{b} Z_v D_v (c_{\infty,v} - c_{0,v}) - \frac{\Omega_i}{b} Z_i D_i c_{\infty,i}, \end{aligned} \tag{13}$$

where $c_{0,v}$ is the equilibrium vacancy concentration in the bulk.

Externally applied stress and the internal stress field of the dislocation microstructure may result in a Peach-Köhler force, which acts on the dislocations. It was shown that the climb force per unit dislocation length F_{cl}, which is the Peach-Köhler force component in the climb direction, controls the equilibrium concentration of vacancies in the vicinity of the dislocation core,[15]

$$c_{d,v} = c_{0,v} e^{-F_{cl}/F_T}, \tag{14}$$

where $F_T = bkT/\Omega_v$. At high temperatures, in which the climb force is much smaller than F_T, the thermal climb rate is approximated to

$$v_{cl,\text{therm}} \approx \frac{2\pi}{\ln(r_\infty/r_d)} \frac{\Omega_v}{b} D_v c_{0,v} \frac{F_{cl}}{F_T}. \tag{15}$$

Under irradiation, dislocations relieve the supersaturation of vacancies and interstitials in the bulk, even without the application of an external force. In the absence of external stress, the irradiation climb rate of an isolated dislocation due to flux of vacancies and interstitials is

$$v_{cl,\text{uncoor}} = \frac{\Omega_v}{b} Z_v D_v (c_{\infty,v} - c_{0,v}) - \frac{\Omega_i}{b} Z_{i,R_0} D_i c_{\infty,i}. \tag{16}$$

We denote this term as "uncoordinated climb", since this result is independent of the surrounding dislocation network. The terms in Eq. (16) depend on the supersaturation of vacancies and interstitials and on the sink strength of an isolated dislocation for interstitials but is independent of the climb force acting on the dislocation.

When an external load is applied, the local strain field in the bulk is a superposition of that of an isolated dislocation and the external strain. Consequently, as seen in Eq. (5), the flux field of interstitials into the dislocation core is altered by the external field, i.e., the capture radius of a dislocation for interstitials varies (we denote the capture radius of the strained dislocation by R and the corresponding sink strength for interstitials by $Z_{i,R}$). Moreover, since different load directions, with respect to the dislocation, lead to the different strain fields, $Z_{i,R}$ depends also on the loading direction. This process, known as the stress induced preferential absorption (SIPA), was suggested by Bullough and Willis,[19] who showed that more interstitials diffuse to edge dislocations with Burgers vectors aligned in the direction of the external stress than into dislocations with Burgers vectors perpendicular to it. They considered it to be one of the underlying mechanisms responsible for irradiation creep. Woo later extended their treatment for a general load direction.[12] It is not surprising, then, that the presence of a dislocation network near the climbing dislocation results in a microstructure-dependent climb rate, due to the strain field induced by the microstructure. In the following, we name that contribution "the coordinated" climb rate. In the next sections, we discuss in detail dislocation climb under irradiation in typical dislocations structures.

III. COORDINATED CLIMB OF DISLOCATIONS

In order to avoid topological difficulties, we deal here with coplanar rectilinear dislocations, i.e., a two-dimensional model and calculate the sink strength of an edge dislocation in a general distribution of edge dislocations. Without loss

of generality, we define the origin of coordinates at the dislocation, whose climb rate we want to calculate, with the Burgers vector aligned along the positive x axis. The other dislocations are distributed all around, at $\mathbf{r_i}$. Accordingly, the strain tensor $\hat{\epsilon}^{\rm tot}$ at each point, outside the dislocation cores, is a superposition of the strain fields of all dislocations

$$\hat{\epsilon}^{\rm tot}(\mathbf{r}) = \hat{\epsilon}^{\rm dis}(\mathbf{r}) + \sum_i \left(\hat{T}_i \cdot \hat{\epsilon}^{\rm dis}(\mathbf{r} - \mathbf{r_i}) \cdot \hat{T}_i^{-1}\right), \qquad (17)$$

where $\hat{\epsilon}^{\rm dis}$ is the strain tensor around an isolated edge dislocation. The strain tensors of all dislocations are rotated to the same coordinate system of the dislocation at the origin (with the rotation matrix $\hat{T}_i$).

In order to calculate the sink strength of the dislocation at the origin, one should employ the general strain field in Eq. (17) with Eq. (5) to express the interaction energy of interstitials with the strain field induced by the dislocation network. However, to our knowledge, there is no analytical solution for the diffusion problem in Eq. (2) with this general interaction energy.

We recall that the strain field of an edge dislocation diverges at the dislocation line and decreases continuously with the distance from it. Thus the contribution of the rest of the network to the strain field near the origin is continuous. If, in addition, the strain field from the surrounding dislocations does not vary strongly near the origin (which may be the case when the dislocation density is low), we may replace the sum in Eq. (17) with a constant strain field $\hat{\epsilon}^{\rm eff}$, which has the value of the superimposed strain fields of the dislocation network at the origin,

$$\hat{\epsilon}^{\rm tot}(\mathbf{r}) \approx \hat{\epsilon}^{\rm dis}(\mathbf{r}) + \hat{\epsilon}^{\rm eff} = \hat{\epsilon}^{\rm dis}(\mathbf{r}) + \sum_i \left(\hat{T}_i \cdot \hat{\epsilon}^{\rm dis}(-\mathbf{r_i}) \cdot \hat{T}_i^{-1}\right). \qquad (18)$$

If we employ the approximate strain field of Eq. (18) in Eq. (5), the interaction energy of an interstitial close to the origin within the strained medium is of the form

$$\psi(\mathbf{r}) = \psi_0 + R(\hat{\epsilon}^{\rm eff})\frac{\sin\theta}{r} + O(r^{-2}), \qquad (19)$$

where ψ_0 is a constant, which does not affect the sink strength. The capture radius R depends on the effective strain $\hat{\epsilon}^{\rm eff}$, i.e., is microstructure dependent. Under the assumption that $R \gg r_d$, the microstructure-dependent sink strength is

$$Z_{i,R}(\hat{\epsilon}^{\rm eff}) = \frac{2\pi}{\ln(2r_\infty/R)}. \qquad (20)$$

In the case where the contribution of the effective strain field to the total strain near the origin is small, the change of the capture radius due to the microstructure is small, and the sink strength can be approximated as

$$Z_{i,R} \approx Z_{i,R_0} + \frac{2\pi}{\ln^2(2r_\infty/R_0)}\left(\frac{R - R_0}{R_0}\right). \qquad (21)$$

From Eq. (21) we identify two contributions to the irradiation climb rate: that which results from the dislocation strain field itself in the absence of other dislocations (*uncoordinated* term) and that which results from the other dislocations (*coordinated* term). We denote this additional contribution to the climb rate, which describes the effect of the strain fields of surrounding dislocations, as *coordinated climb*,

$$v_{cl,\rm coor} = -\frac{\Omega_i}{b}\left(Z_{i,R} - Z_{i,R_0}\right) D_i c_{\infty,i}. \qquad (22)$$

To summarize, the total climb rate is the sum of the thermal climb rate [Eq. (15)], the uncoordinated climb rate [Eq. (16)], and the coordinated climb rate [Eq. (22)]. In what follows, we shall examine the contribution of coordinated climb to some ordered dislocation structures.

IV. COORDINATED CLIMB OF DISLOCATION PAIRS

Edge dislocations of opposite sign on different slip planes may annihilate via dislocation climb (Fig. 1). In the configuration sketched on Fig. 1, elastic interaction between the two dislocations is attractive: thermal climb alone promotes annihilation. Irradiation accelerates this process if it increases the climb rate of dislocations one toward the other. If we were to treat dislocations as isolated, the rate of decrease of the dislocation spacing would be reduced (respectively enhanced) for the configuration given in Fig. 1(a) [respectively 1(b)] if the flux of interstitials to each individual dislocation is larger

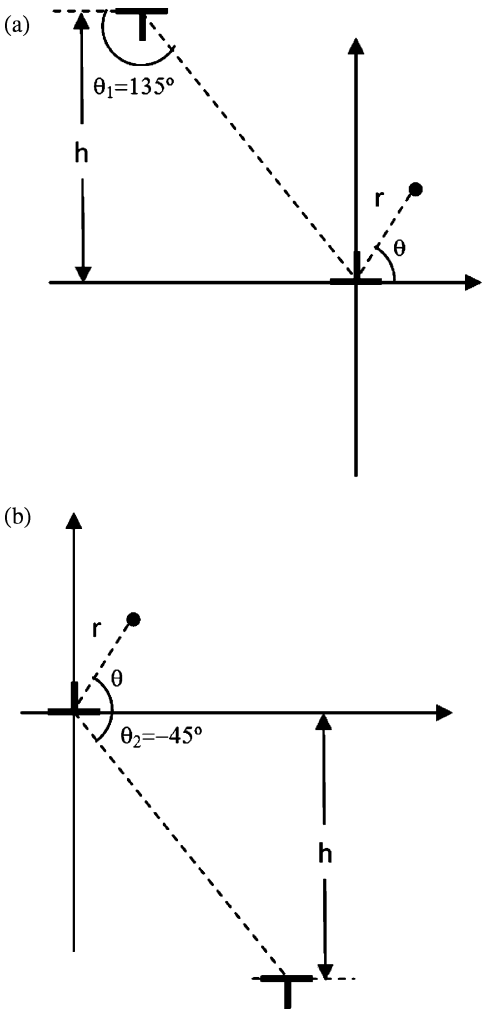

FIG. 1. Two different configurations of dislocation pairs at equilibrium positions.

than that of vacancies, which is usually the case. We show herein that, at variance, coordinated climb always enhances the annihilation rate.

First, we consider a stable structure of a dislocation pair in which the line connecting the dislocations is at 45° from their slip plane (Fig. 1). We distinguish between two cases, marked as (a) and (b) in Fig. 1. In both cases, the distance between the slip planes is h. Due to symmetry, it is sufficient to calculate the sink strength of one of the dislocations. Without loss of generality, we locate the dislocation, the climb rate of which we want to calculate, at the origin; its Burgers vector is in the positive x direction. Then the second dislocation is either at $\theta_1 = 135°$ or $\theta_2 = -45°$ with the positive x axis (see Fig. 1). Denoting the distance and the angle from the origin as r and θ, we approximate the contribution of the second dislocation by an effective constant strain field—the value of its strain tensor at the origin,

$$\epsilon_{ij}^{\text{pair}}(r,\theta) = \epsilon_{ij}^{\text{dis}}(r,\theta) + T_{ik}\epsilon_{kl}^{\text{dis}}(\sqrt{2}h,\theta')T_{jl}, \tag{23}$$

where $\theta' = \theta_1$ or $\theta' = \theta_2$, depending on the structure. The xx and yy components of the effective strain tensor are described in Fig. 2.

If we employ the isotropic elasticity theory of dislocations (see the Appendix) and we substitute Eq. (23) in Eq. (5), we find that the interaction energy of interstitials with the strain field of the dislocation at the origin, in the presence of the second dislocation, is

$$\psi(\mathbf{r}) = \psi_0 + R_0\left(1 \mp \kappa_{\text{pair}}\frac{b}{h}\right)\frac{\sin\theta}{r} + O(r^{-2}). \tag{24}$$

The $\mp$ refers to the dislocation configurations in Figs. 1(a) and 1(b), respectively. In Eq. (24), we replaced $\cos^2\theta$ and $\sin^2\theta$ by their mean value and we retained only contributions up to the order of r^{-1}, similarly to the analysis by Bullough and Willis.[19] κ_{pair} is a dimensionless factor

$$\kappa_{\text{pair}} = -\frac{\sqrt{2}}{2\pi\Omega_i K\epsilon^{\text{misfit}}}\frac{1-2\nu}{1-\nu}\left(\alpha^K + \frac{2(\nu^2-\nu+1)}{3(1-2\nu)^2}\alpha^G\right). \tag{25}$$

We would like to emphasize this result. When considering each dislocation individually, the capture radius of each dislocation in the dislocation pair structure is R_0. When considering the coordinated climb contribution, the inhomogeneity of the interstitial strain field contributes to the climb rate, in a way that depends on the pair structure. In particular, the coordinated climb contribution increases as the distance between the dislocation decreases, at variance with the uncoordinated term.

If we adopt negative values for α^G and α^K, as suggested by Wolfer,[14] κ_{pair} is positive. As an example, using parameter values typical of Cu (see Table I), we find that $\kappa_{\text{pair}} = 0.43$. For positive values of κ_{pair}, the capture radii decrease in the case described in Fig. 1(a). This leads to the smaller fluxes of interstitials into the dislocations, which results in annihilation rates that are faster than predicted when omitting the coordinated term. In the second case [Fig. 1(b)], the capture radii increase, as does the interstitial flux to each dislocation, and the dislocation pair annihilates faster as well. To summarize, the coordinated climb term positively contributes to the annihilation rates under irradiation of dislocation pairs with opposite signs.

This result can be understood in the framework of SIPA. Since the stress field of each dislocation is asymmetric about its glide plane, the dislocation at the origin is in the compression or tension area of the second dislocation, depending on the

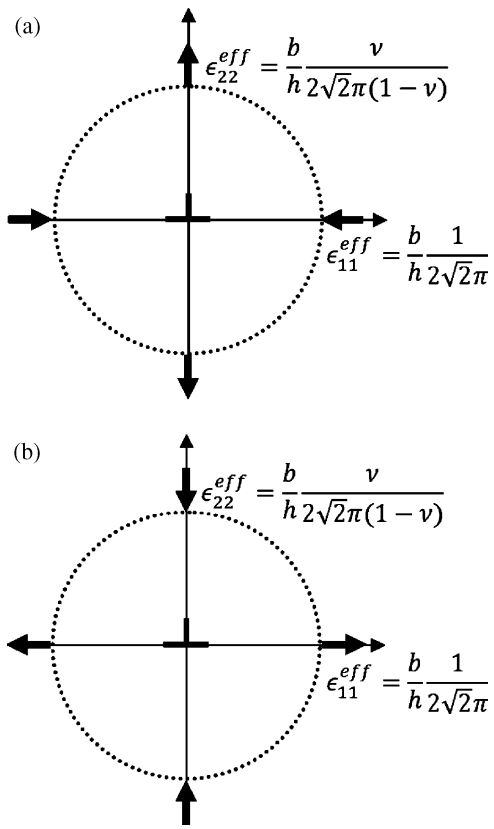

FIG. 2. The effective strain applied on a dislocation in a dislocation pair structure by its counterpart. (a) and (b) refer to dislocation structures in Fig. 1.

TABLE I. Bulk and self-interstitial elastic properties of Cu.

Parameter	Value
G[a]	54.6 GPa
K[a]	136.9 GPa
ν[a]	0.324
Ω[a]	11.8 Å^3
Ω_v/Ω[b]	0.9
ϵ^{misfit}[c]	1.45
α^G[c]	−34.4 eV
α^K[c]	−24.0 eV
$D_s(T)$[d]	$0.2e^{-5667.208/T}$ cm^2/sec
f[e] (in fcc)	0.781

[a]Taken from Ref. 15.
[b]Reference 30.
[c]Reference 14.
[d]Reference 31.
[e]Reference 24.

type of dislocation pair. It is then not surprising that the underlying principles of SIPA rationalize the different capture radii between both cases. It is important to note that the coordinated climb term is related to the anisotropic properties of the dumbbell interstitial in the matrix. The interstitial elastic inhomogeneity gives rise to additional terms in the interaction energy between the interstitial and the strain fields of both dislocations *simultaneously*, which are of the same order of magnitude as the size effect. This term breaks down the symmetry of the problem and changes the dislocation's sink strength for interstitials. Considering only the dilatation term in the interaction energy is insufficient and will lead to structure-independent capture radii (which are equal to that of an isolated dislocation).

V. ANNIHILATION OF DISLOCATION DIPOLES

A. Sink strength of dislocations in a dipole structure

If both dislocations share the same climb plane (as in Fig. 3), we would call that a dislocation dipole. The two-dimensional dipole structures are indeed unstable due to a component of the Peach-Köhler force in the glide direction. However, these structures are a two-dimensional representation of three-dimensional elongated dislocation loops. We omit the possible glide motion of the dislocations in this structure.

As in dislocation pairs, we differentiate between two cases, which we denote as interstitial and vacancy dipoles, where a ribbon of atoms is being added or removed in the climb plane between the dislocations (see Fig. 3 for an example of a vacancy dipole). Figure 3 also exhibits the strain field around one of the dislocations in the dipole structure. It emphasizes our assumption that its contribution to the sink strength of the second dislocation can be approximated by a constant strain field. Each dislocation in a vacancy-type dipole is in the tensile region of the elastic field produced by its counterpart; at variance, each dislocation in an interstitial-type dipole is

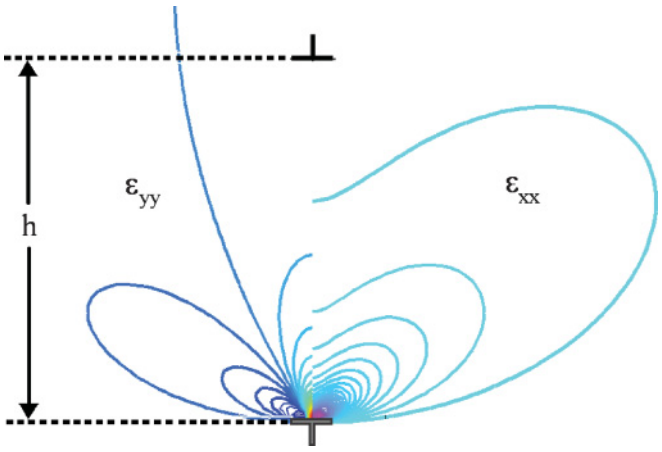

FIG. 3. (Color online) A vacancy type dislocation dipole of size $h = 50b$. Contours of two strain components of the bottom dislocation are sketched (ϵ_{xx} on the right and ϵ_{yy} on the left). We notice that the upper dislocation, the sink strength of which we want to calculate, is located in the tension region of its counterpart, but the strain there is not varying strongly, which allows us to approximate it as a constant.

under compression. Therefore, due to strain field resulting at each dislocation, the sink strength for interstitials of each dislocation depends on the configuration of the dipole, and in all cases differs from that of an isolated dislocation.

The effective strain is calculated in a similar manner to that of dislocation pairs [Eq. (23)], with now $\theta_1 = 90^\circ$ or $\theta_2 = -90^\circ$. As a result, a form of interaction energy similar to Eq. (24) is found (see the Appendix), with different capture radii

$$R = R_0 \left(1 \mp \kappa_{\text{dipole}} \frac{b}{h}\right), \tag{26}$$

where κ_{dipole} is

$$\kappa_{\text{dipole}} = -\frac{1}{\pi \Omega_i K \epsilon^{\text{misfit}}} \frac{1-2\nu}{1-\nu} \left(\alpha^K + \frac{1}{6}\alpha^G\right). \tag{27}$$

The $\mp$ sign refers to interstitial and vacancy dipoles, respectively. If we employ parameters values typical of Cu (Table I), we find that $\kappa_{\text{dipole}} = 0.66$. As was the case for dislocation pairs, the capture radius differs between interstitial and vacancy dipoles, but the coordinated climb contribution always accelerates dipole annihilation. Let us estimate quantitatively the annihilation rate in two limits, $R \ll h \ll r_\infty$ and $h \ll R$.

B. Dipole annihilation rate when $R \ll h \ll r_\infty$

For the constant effective strain approximation in Eq. (18) to hold, the capture radii around the dislocations should not overlap (we further assume herein that $R \ll h$). In order to explicitly calculate the annihilation rate, one should adopt a similar approach to that suggested in Ref. 15 for the annihilation of vacancy dipole via thermal climb. It was emphasized there that the diffusion equation should be solved simultaneously in the presence of both dislocations and not around each dislocation separately. Roughly, one can postulate that the climb rate is decreased by a factor of 2 (point defects from the area surrounding the dipole diffuse into both dislocations, reducing the flux into each one by a factor 2). While better approximation can be done, the solution for interstitials is rather tedious, and postulating a factor of 2 is sufficient to capture the essential features. We also neglect recombination of vacancies and interstitials near the dislocations, and we hypothesize that the supersaturations in the bulk remain constant. Under these assumptions, the shrinkage/expansion rate of vacancy dipoles is

$$\dot{h}_{vd} = \frac{\Omega_v}{b} Z_v D_v (c_{\infty,v} - c_{d,v}) - \frac{\Omega_i}{b} Z_i^{vd} D_i c_{\infty,i}, \tag{28}$$

and that of interstitial dipoles is

$$\dot{h}_{id} = -\frac{\Omega_v}{b} Z_v D_v (c_{\infty,v} - c_{d,v}) + \frac{\Omega_i}{b} Z_i^{id} D_i c_{\infty,i}, \tag{29}$$

where Z_i^{vd} and Z_i^{id} are the sink strengths of dislocations in vacancy and interstitial dipoles, respectively [in correlation with the sink strengths R found in Eq. (26)]. In the above expressions, we distinguish the contributions of the thermal, the uncoordinated, and the coordinated terms.

In both cases, the dislocations attract each other with a climb force per unit dislocation length of $|F_{cl}| = \mu b^2/2\pi(1-\nu)h$. In the case of a vacancy dipole, in the absence of irradiation ($c_{\infty,v} = c_{0,v}$ and $c_{\infty,i} = 0$), this climb force tends to increase

the vacancy equilibrium concentration near the dislocation core and vacancies diffuse outward from dislocations, thus promoting shrinkage. In interstitial dipoles, the climb force stimulates inward vacancy flux, which also results in annihilation of the dipole structure. We note that the value of $c_{d,v}$ is different between Eqs. (28) and (29), because of the direction of the climb force, relative to the dislocation.[22] If we consider the sink strength for vacancies in Eq. (4) and we assume that $|F_{cl}| \ll F_T$, the thermal contribution is identical for both types of dipoles,

$$\dot{h}_{vd,\text{therm}} = \dot{h}_{id,\text{therm}} = -\frac{2\pi}{\ln(r_\infty/r_d)}\frac{\Omega_v}{b}D_v c_{0,v}\frac{\mu\Omega_v}{2\pi kT(1-\nu)}\left(\frac{b}{h}\right). \quad (30)$$

The uncoordinated contribution is structure independent. However, the same fluxes lead to opposite climb directions between vacancy (vd) and interstitial dipoles (id), which results in the following contribution:

$$\dot{h}_{vd,\text{uncoor}} = -\dot{h}_{id,\text{uncoor}} = \frac{2\pi}{\ln(r_\infty/r_d)}\frac{\Omega_v}{b}D_v(c_{\infty,v}-c_{0,v}) - \frac{2\pi}{\ln(2r_\infty/R_0)}\frac{\Omega_i}{b}D_i c_{\infty,i}. \quad (31)$$

On the contrary, the coordinated climb rate is structure dependent. We recall that the interstitial flux into an interstitial dipole decreases and, as a result, the dislocations climb faster one toward the other, while into a vacancy dipole the flux increases, which also results in faster shrinkage rate. Employing the capture radii found in Eq. (26) in Eq. (22), the coordinated term is

$$\dot{h}_{vd,\text{coor}} = \dot{h}_{id,\text{coor}} = -\frac{2\pi}{\ln^2(2r_\infty/R_0)}\frac{\Omega_i}{b}\kappa_{\text{dipole}}D_i c_{\infty,i}\left(\frac{b}{h}\right). \quad (32)$$

It is clear from this result that the contribution of the coordination term has the same tendency as the thermal contribution. Both thermal climb and coordinated irradiation climb tend to decrease the dipole width, with an increasing rate as the dipole becomes narrower.

C. Annihilation rate of dipoles with size $h \ll R_0$

When the capture radii of both dislocations in the dipole structures overlaps $h \ll R_0$, the assumption made in this work, that the strain field of the microstructure can be replaced by an effective constant one, becomes inaccurate. In this case, the dislocations are no longer treated as two independent sinks for interstitials. Instead, the strain field of both dislocations should be considered simultaneously. However, at a distance $r \gg h$, the strain field of the dipole is short ranged and as opposed to an isolated dislocation, the first significant contribution is of the order of r^{-2} (r is the distance from the center of the dipole).[14] Thus the contribution of the interaction energy of interstitials with the dislocation dipole is weak and can be neglected (which is evident in the extreme case of h approaching 0, in which the strain field of the dipole vanishes). In this case, the sink strength for interstitials approaches that for vacancies as the dipole becomes narrower and the shrinkage/expansion rate of very narrow dipoles is

$$\dot{h}|_{h\ll R_0} = \pm\frac{2\pi}{\ln(r_\infty/r_d)}\frac{\Omega}{b}[D_v(c_{\infty,v}-c_{d,v}) - D_i c_{\infty,i}]. \quad (33)$$

The $\pm$ refers to vacancy and interstitial dipoles, respectively. For our discussion, it is sufficient to consider that $\Omega_i \approx \Omega_v$ (which we denote as Ω). If we assume irradiation in stationary conditions $D_i c_{\infty,i} \approx D_v c_{\infty,v}$ in Eq. (33), only the thermal part is retained,

$$\dot{h}|_{h\ll R_0} = -\frac{2\pi}{\ln(r_\infty/r_d)}\frac{\Omega}{b}D_v c_{0,v}\frac{\mu\Omega_v}{2\pi kT(1-\nu)}\left(\frac{b}{h}\right). \quad (34)$$

To summarize, as the dipole becomes narrow, the coordinated term competes with the uncoordinated term and the total contribution of the irradiation diminishes.

VI. COORDINATED CLIMB OF DISLOCATIONS IN AN EDGE DISLOCATION WALL

A. Two dislocations with the same sign under irradiation

In the case of same sign dislocations, aligned on parallel slip planes and constrained by some external field to lie on the same climb plane (see Fig. 4), elasticity theory predicts a repulsion force between them, which results in a climb force in opposite directions for each dislocation. Hence climb will increase the distance between them. When the neighboring dislocation is not taken into account, irradiation does not promote any increase in distance, since its contribution to the

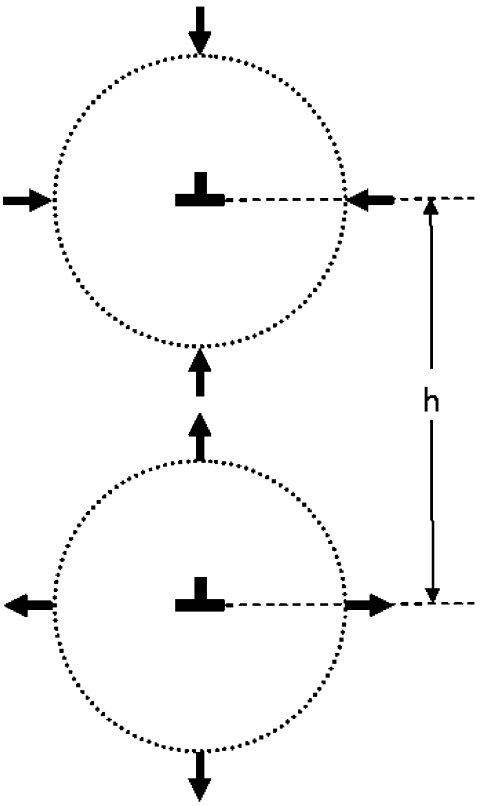

FIG. 4. The effective strain fields applied on dislocations of the same sign by their counterparts. Notice that the upper dislocation is under compression and the bottom one is under tension.

climb rate of each dislocation (treated as being isolated) is the same.

However, when accounting for the coordination term, one should notice that the upper dislocation is in the compression region of the lower one, while the lower dislocation is in the tension region of the upper one. This difference leads to different sink strengths for interstitials. Similar treatment as in the previous section yields for the capture radii of the upper and lower dislocations:

$$R_{\text{upper}} = R_0\left(1 - \kappa_{\text{dipole}}\frac{b}{h}\right),$$
$$R_{\text{lower}} = R_0\left(1 + \kappa_{\text{dipole}}\frac{b}{h}\right). \tag{35}$$

As a result, the contributions of the various climb mechanisms to the evolution of the distance between dislocations are

$$\dot{h}_{\text{therm}} = \frac{2\pi}{\ln(r_\infty/r_d)}\frac{\Omega_v}{b}D_v c_{0,v}\frac{\mu\Omega_v}{2\pi kT(1-\nu)}\left(\frac{b}{h}\right),$$
$$\dot{h}_{\text{uncoor}} = 0, \tag{36}$$
$$\dot{h}_{\text{coor}} = \frac{2\pi}{\ln^2(2r_\infty/R_0)}\frac{\Omega_i}{b}\kappa_{\text{dipole}}D_i c_{\infty,i}\left(\frac{b}{h}\right).$$

This result is fundamentally different from the previous case of dislocation dipoles. The directionality in the edge dislocation's strain field promotes a higher interstitial flux to the lower dislocation than to the upper one. Consequently, the coordinated term enhances the rate at which dislocations climb away from one another—a unique contribution of irradiation that is not predicted if we consider only the uncoordinated term.

As in the case of dislocation dipoles and pairs, the directions of coordinated and thermal climb are the same. The ratio between the contributions of thermal and coordinated climb is independent of the distance between dislocations,

$$\frac{\dot{h}_{\text{coor}}}{\dot{h}_{\text{therm}}} = \frac{\ln(r_\infty/r_d)}{\ln^2(2r_\infty/R_0)}\frac{\Omega_i}{\Omega_v}\frac{2\kappa_{\text{dipole}}\pi kT(1-\nu)}{\mu\Omega_v}\frac{D_i c_{\infty,i}}{D_v c_{0,v}}. \tag{37}$$

Considering the values for Cu (in Table I) at half the melting temperature, the contributions of thermal and coordinated climb are of equal importance if the level of supersaturation satisfies that $D_i c_{\infty,i}$ is two orders of magnitude larger than $D_v c_{0,v}$. The relative contribution of coordinated climb becomes even more important at higher irradiation dose rates (higher drift forces of interstitials) or at lower temperatures (interstitials are more mobile than vacancies). Thus coordinated climb contribution prevails at low-intermediate temperatures and at intermediate-high irradiation fluxes.

Under such conditions, our model predicts that the coordinated climb becomes the dominant process: irradiation induced coordinated climb will speed up the annealing of the dislocation network, in agreement with the observation by Maziasz in 300 series austenitic stainless steels.[5] We generalize this conclusion and suggest that irradiation has a non-negligible contribution to the annealing of dislocation structures, which adds to the thermal contribution, with a completely distinct temperature dependence.

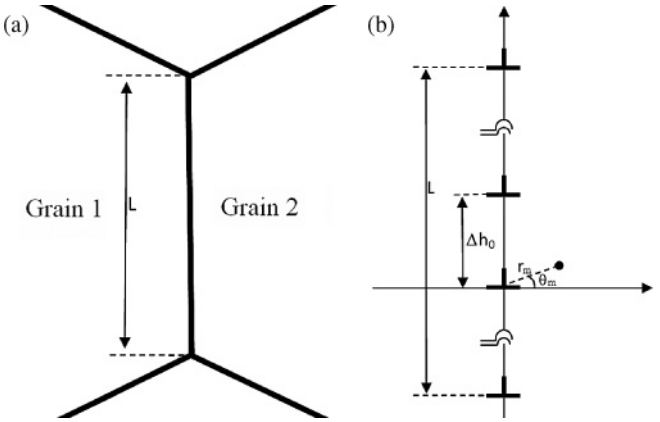

FIG. 5. (a) A low-angle tilt boundary of a finite length size L between two grains. (b) The dislocation configuration in the finite length wall. The origin of coordinates is defined at the m^{th} dislocation.

B. Climb of dislocations in a finite-size dislocation wall (a disclination dipole)

We extend our discussion of same sign dislocations to the irradiation-driven evolution of a low-angle tilt boundary of a finite length size L, as sketched in Fig. 5(a). Similar to the analysis of two dislocations with identical sign, elasticity theory predicts a repulsion force between the dislocations the wall is made of. This force allows thermal climb to increase the interdislocation spacing hence favoring restoration by grain rotation across the tilt boundary.[23] We show here that coordinated climb under irradiation has an additional contribution to grain rotation.

We denote the initial separation distance between dislocations within the wall as Δh_0 [which refers to an initial misorientation angle of $\chi_0 = b/\Delta h_0$ (Ref. 15)]. For convenience, we choose a wall size, which is represented by an odd number of dislocations $2N_0 + 1$, and we number the dislocations from $-N_0$ at the bottom to N_0 at the top [Fig. 5(b)]. Further, we shall discuss the case of large N's, which is the case of a long boundary. The strain field in the vicinity of the m^{th} dislocation, at a distance r_m and an angle θ_m, is a superposition of its strain field and a uniform effective strain field, which includes contributions from all the other dislocations,

$$\epsilon_{ij}^{\text{wall}}(r_m,\theta_m) = \epsilon_{ij}^{\text{dis}}(r_m,\theta_m) + \sum_{n=-N_0,n\neq m}^{n=N_0}\epsilon_{ij}^{\text{dis}}\left(|m-n|\,\Delta h_0, \text{sgn}(m-n)\frac{\pi}{2}\right). \tag{38}$$

Notice that each dislocation is in the tensile region of the dislocations above it, and under compression from the dislocations below. Thus the effective strain field at each dislocation, from the neighboring dislocations that construct the wall [see Eq. (18)], depends on its position along the wall.

It can be shown[15] that the sum in Eq. (38) can be replaced with an effective strain field of a single dislocation at an effective distance $|H_m|$ above ($H_m > 0$) or below ($H_m < 0$) the m^{th} dislocation, of the same sign as the m^{th} dislocation:

$$\epsilon_{ij}^{\text{wall}}(r_m,\theta_m) = \epsilon_{ij}^{\text{dis}}(r_m,\theta_m) + \epsilon_{ij}^{\text{dis}}\left(|H_m|, \text{sgn}(H_m)\frac{\pi}{2}\right). \tag{39}$$

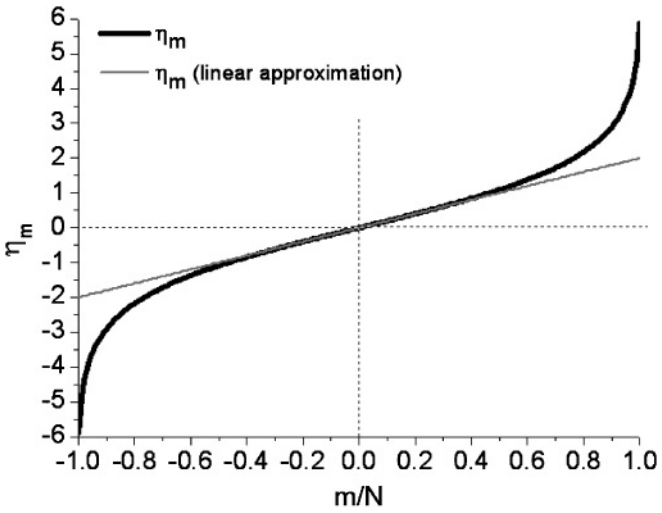

FIG. 6. The value of η_m [Eq. (40)] along a finite length dislocation wall, as a function of the relative position along the wall. The linear approximation, which is employed in this work, is also plotted.

H_m satisfies

$$\frac{1}{H_m} = \frac{1}{\Delta h_0} \sum_{n=-N_0, n\neq m}^{n=N_0} \frac{1}{n-m} = \frac{\eta_m}{\Delta h_0}; \tag{40}$$

η_m is an antisymmetric monotonic ascending function of m (see Fig. 6). If we employ Eq. (35) for dislocations of the same sign at a distance H_m, we find that the capture radius of the m^{th} dislocation for interstitials is

$$R_m = R_0 \left(1 - \kappa_{\text{dipole}} \eta_m \frac{b}{\Delta h_0}\right), \tag{41}$$

where κ_{dipole} is given in Eq. (27). Since $\kappa_{\text{dipole}} > 0$, the sink strength for interstitials along the wall distributes monotonically, whereas the lowest and uppermost dislocations have the strongest and weakest sink strengths, respectively. The dislocation at the center has the same capture radius as an isolated dislocation. Since interstitials are absorbed more efficiently at the lower part of the wall than in the upper part, the dislocations are climbing away from each other. As a result, irradiation increases the length of the disclination dipole.

In the limit of large N's, η_m approaches the function $\eta_m = 2\text{arctanh}(m/N_0)$. At the center of the wall, this function is approximately linear (see Fig. 6) and the capture radius of the m^{th} dislocation can be approximated to

$$R_m \approx R_0 \left(1 - \kappa_{\text{dipole}} \frac{2m}{N_0} \frac{b}{\Delta h_0}\right). \tag{42}$$

Since the distribution of the sink strength depends on the *relative* position inside the wall (m/N_0), the larger the wall is, the longer the region in the middle of the wall where the sink strength is linearly distributed. Thus regardless of the wall length, the distance between dislocations in a low-angle tilt boundary is expected to increase under irradiation, which will result in a decrease of the misorientation across the boundary.

As for the thermal contribution, similar analysis shows that the climb force applied on each dislocation by the neighboring ones varies along the wall. The dislocations at the lower half are repelled downward, while those on the upper half are pushed upward. As a result, the dislocations at the lower part climb by emitting vacancies to the bulk while the upper ones climb by vacancy absorption. It can be shown that the climb force on the m^{th} dislocation is

$$F_{cl,m} = \frac{\mu b \eta_m}{2\pi(1-\nu)} \frac{b}{\Delta h_0} \approx \frac{\mu b}{\pi(1-\nu)} \frac{m}{N_0} \frac{b}{\Delta h_0}. \tag{43}$$

The climb force promotes dislocations to climb away from each other under thermal conditions, resulting in thermal subgrain growth.

C. Irradiation-driven grain rotation

In order to estimate the rotation rate of two adjacent subgrains, under irradiation, let us calculate the distribution of climb rates along the disclination dipole. Two processes contribute to an increase in the length of the disclination dipole: thermal climb due to the climb component of the Peach-Köhler forces and the coordinated climb term; the uncoordinated term does not contribute, since it has a uniform contribution along the wall, regardless of the location of the dislocation along the wall.

The wall has no long-range strain field associated to it: the latter decays exponentially away from the wall, with a decay length of the order of the dislocation spacing Δh_0. Accordingly, we shall assume that the concentration of point defects on the boundaries of a slab of width Δh_0 around the wall is homogeneous c_{wall}. In the case of irradiation, the concentration gradient from the bulk into the slab on the wall results in a homogeneous flux of point defects into the wall. Inside the slab, the coordinated climb redistributes the point defects due to the internal strain inside the wall. Thus the climb rate of the m^{th} dislocation is

$$v_{cl,m} = \frac{\Omega_v}{b} Z_v D_v (c_{\text{wall},v} - c_{m,v}) - \frac{\Omega_i}{b} Z_{m,i} D_i c_{\text{wall},i}. \tag{44}$$

We denote the sink strength for interstitials of the m^{th} dislocation as $Z_{m,i}$ and the equilibrium vacancy concentration at the m^{th} dislocation as $c_{m,v}$. We emphasize that since we separated the problem into two parts: outer flux to the slab, and redistribution inside the slab, each dislocation is treated separately with $r_\infty = \Delta h_0/2$.

When we address the evolution of a grain boundary between two grains in the bulk, the model presented here does not treat correctly the strain field near the triple junctions. In an actual polycrystal, grain boundaries merge at triple junctions; each finite length boundary is indeed a disclination dipole, with the singularity at the two wall edges, compensated by that of the boundaries, which merge at the triple junctions. Full relaxation only occurs if the rotations of all the grains are coordinated. In the general case, the stress on the dislocations at the edges is difficult to estimate. Consequently, we estimate here the evolution of the distance between dislocations at the center of wall, in order to avoid the inaccuracy of our treatment at the terminal dislocations. We then assume that the linear approximation in Eq. (42) extends along the whole wall. Under this approximation, the difference between the climb rates of two neighboring dislocations is

$$\Delta v_{cl} = \frac{\Omega_v}{b} Z_v D_v \Delta c_v - \frac{\Omega_i}{b} \Delta Z_i D_i c_{\text{wall},i}, \tag{45}$$

where Δc_v and ΔZ_i are, respectively, the differences in the vacancy concentration in the vicinity of two neighboring dislocations and the difference in their sink strength for interstitials. These parameters are independent of the position of the pair of dislocations along the wall.

If $r_\infty \gg R_{m,i} \gg r_d$, the sink strength is varying slowly along the disclination dipole and the difference in sink strengths between two neighboring dislocations can be approximated by Eqs. (21) and (41),

$$\Delta Z_i = -\frac{4\pi\kappa_{\text{dipole}}\chi}{\ln^2(2r_\infty/R_0)}\frac{1}{N}. \tag{46}$$

We note that the grain-boundary size $L = 2N_0\Delta h_0 = 2N\Delta h$ is conserved during grain rotation: notice that N and χ are now functions of time, unlike N_0 and χ_0. In addition, according to Eqs. (14) and (43), the difference in the equilibrium vacancy concentrations in the vicinity of two neighboring dislocations is

$$\Delta c_v = \frac{\mu\Omega_v\chi}{\pi(1-\nu)kT}\frac{1}{N}c_{0,v}. \tag{47}$$

The average distance between dislocations increases in time at a rate that is equal to

$$\frac{d(\Delta h)}{dt} = \Delta v_{cl}. \tag{48}$$

Replacing the distance between neighboring dislocations by the misorientation angle of the boundary $\chi = b/\Delta h$, a differential equation for χ is found by substituting Eqs. (45)–(47) in Eq. (48),

$$\dot{\chi} = -\frac{4\pi}{bL}\left[\frac{1}{\ln(r_\infty/r_d)}\frac{\mu\Omega_v}{\pi(1-\nu)kT}\Omega_v D_v c_{0,v} + \frac{2}{\ln^2(2r_\infty/R_0)}\kappa_{\text{dipole}}\Omega_i D_i c_{\text{wall},i}\right]\chi^2. \tag{49}$$

We employed the fact that N is varying with time, and replaced it with boundary length $L = 2Nb/\chi$. If we neglect the dependency of $\ln(r_\infty/r_d)$ on Δh (a slowly varying quantity), the solution of this equation satisfies

$$\frac{1}{\chi} = \frac{1}{\chi_0} + \frac{t}{\tau}, \tag{50}$$

with a characteristic time τ for grain rotation, which satisfies

$$\tau^{-1} = \frac{4\pi}{bL}\left[\frac{1}{\ln(r_\infty/r_d)}\frac{\mu\Omega_v}{\pi(1-\nu)kT}\Omega_v D_v c_{0,v} + \frac{2}{\ln^2(2r_\infty/R_0)}\kappa_{\text{dipole}}\Omega_i D_i c_{\text{wall},i}\right]. \tag{51}$$

The higher τ is, the slower the grain rotation, which results in a decrease of the energy of the sub-boundary. From this result one can see that high supersaturation of interstitials near the wall, fast diffusion, or large elastic inhomogeneity of the interstitial in the matrix (large κ_{dipole}) lead to small τ's, i.e., high rotation rates. It is interesting to note that the supersaturation of vacancies will not stimulate grain rotation since it is relieved by diffusing homogeneously into the dislocations constituting the wall.

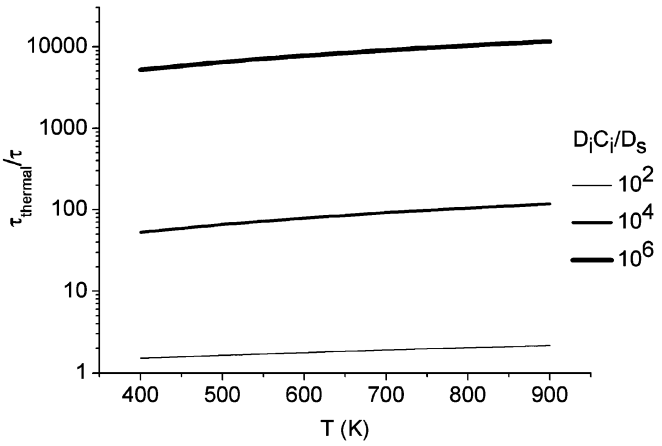

FIG. 7. The decrease in the characteristic time τ for grain rotation under irradiation as a function of temperatures for various supersaturations of interstitials.

We estimate the contribution of irradiation to the grain rotation. Under nonirradiation conditions ($c_{\infty,v} = c_{0,v}$ and $c_{\text{wall},i} = 0$), the characteristic time for grain annealing is

$$\tau_{\text{therm}} = \frac{bL}{4\pi}\ln(r_\infty/r_d)\frac{\pi(1-\nu)kT}{\mu\Omega_v}\frac{1}{\Omega_v D_v c_{0,v}}. \tag{52}$$

Under irradiation, the grain boundary relaxes faster (lower τ). The decrease in the characteristic relaxation time, associated to the elimination of irradiation produced defects at the grain boundary, is

$$\frac{\tau_{\text{therm}}}{\tau} = 1 + 2\frac{\ln(r_\infty/r_d)}{\ln^2(2r_\infty/R_0)}\frac{\pi(1-\nu)kT}{\mu\Omega_v}\frac{\Omega_i}{\Omega_v}\kappa_{\text{dipole}} f\frac{D_i c_{\infty,i}}{D_s}. \tag{53}$$

Since the strain field of the grain boundary is short ranged, we hypothesize the interstitials' concentration to be homogeneous within the grain so that $c_{\text{wall},i} \approx c_{\infty,i}$. We replaced $D_v c_{0,v}$ with D_s/f, where D_s is the self-diffusion coefficient and f is the Bardeen-Herring correlation factor for solvent diffusion.[24] It is important to note that the relative time for grain annealing, with respect to thermal annealing, is independent of the boundary length (which corresponds to the grain size), i.e., irradiation accelerates the rotation of all grains, whatever the sizes, in the same proportion. In Fig. 7 we plot how much τ is reduced due to irradiation in Cu [Eq. (53)], as a function of temperature, for various irradiation conditions. We employed the parameters in Table I. One can see that at low irradiation induced defect supersaturation, the effect of irradiation is not substantial. However, for a defect supersaturation by four orders of magnitude (as measured by $D_i c_{\infty,i}/D_s$) we predict a two orders of magnitude decrease of the characteristic time for grain rotation. However, we recall that in order to perform a realistic quantitative evaluation of the relaxation time in an actual material, one needs to compute carefully the irradiation parameters, in particular $D_i c_{\infty,i}$ which depends on all the components of the microstructure (Ref. 25).

VII. DISCUSSION AND SUMMARY

We find that the rate of change of the dislocation spacing under irradiation due to climb, in the various cases of

dislocation structures considered in this work, comprises three contributions:

(1) A thermal climb contribution, identical to that which prevails in the absence of irradiation. The latter drives the dislocation network to lower strain energy, by annihilating dipoles made of dislocations with opposite signs and by making dislocation of the same sign climb away. The rate of this first contribution is proportional to $D_v c_{0,v}$, regardless of the irradiation conditions.

(2) An uncoordinated contribution, which, depending on the configuration of the dislocations, may either decrease or increase the strain energy of the network, by forcing climb in a direction independent of the sign of the climb force.

(3) A coordinated contribution, the result of which adds to that of the thermal contribution, but with a rate proportional to $D_i c_{\infty,i}$. This SIPA-like contribution promotes irradiation enhanced climb, which eventually results in the disappearance of the initial microstructure.

To summarize, the competition between annihilation of dislocations structures under irradiation, multiplication of dislocation via climb sources and the agglomeration of point defects into dislocations leads to the recovery of the initial dislocation network and the nucleation of a dislocation loops population, which eventually grow into a new *stationary* dislocation network, independently of the initial network.

The magnitude of the effect of coordinated climb on the annihilation of dislocation structures was demonstrated for Cu. Our numerical examples were limited to Cu, due to the availability of the data on interstitials' elastic properties. In the future, we plan on performing atomistic simulations to study these elastic properties in other metals that are in use in the nuclear industry (Fe, in particular).

In this work we assumed quasistationary conditions for the defect concentration fields, i.e., that the average concentrations of point defects in the bulk remain unaltered by the microstructural evolution. However, the microstructure is made of the grain boundaries, the dislocation network, and defect clusters of various types (interstitial loops, cavities, bubbles, stacking fault tetrahedra), each of which with its own sink strength.[25] We assumed that the sink strengths change slowly in time, due to defect accumulation on each sink; at each time, the defect concentration can be considered as stationary with respect to the microstructure. However in reality, both $c_{\infty,v}$ and $c_{\infty,i}$ evolve in the course of irradiation, due to the slow evolution of the defect sink structure in the material. A detailed calculation of each of the above terms can be performed, provided that the microstructure is quantified into details (grain size, dislocation density, number density, and size of various defect clusters, acting as defect sinks). For the time being, we focused on demonstrating the effects of the mechanisms we propose, leaving detailed applications for future work.

While the time evolution of the loop population can be modeled easily, using the rate theory for defect accumulation,[26,27] it is not the case for the time evolution of the initial network: the complexity of the three-dimensional arrangement of the dislocation lines, together with the topological constraints that prevail when dislocations merge, even without irradiation, makes the modeling difficult. This difficulty is well known in the community of crystalline plasticity (e.g., Ref. 28). The complexity is increased under irradiation, where dislocation climb becomes a key contribution. Computer simulation of the evolution of the dislocation network, based on discrete dislocation dynamics (DDD) technique, allow us to circumvent the modeling difficulty, provided dislocation climb is included as an active process. Recently, DDD simulations have addressed the problem of climb due to vacancy diffusion,[22,29] which is appropriate to simulate thermal creep. Such developments should now be extended to self-interstitials in order to cope with the evolution of the microstructure under irradiation. While we have provided here examples of two-dimensional structures of straight dislocations, our approach is suitable for such developments of three-dimensional DDD simulations at intermediate-high temperatures (dislocations are highly jogged) and when pipe diffusion can be omitted. These simulations would make it possible to simulate irradiation creep in single crystals.

In our model, we replaced the general strain field of the surrounding microstructure with a constant strain field. This approach can be extended to a general strain field [Eq. (17)], in order to obtain an accurate numerical solution for a general geometry of dislocations and grain boundaries. Such an extension can be coupled with numerical methods to study polycrystalline material properties, such as that proposed by Moretti *et al.*[32] In this work, the authors adapted the description of the vortex lattice to treat grain boundaries in polycrystalline material in the framework of elasticity theory of dislocations.[32] The re-arrangement of the grain boundary in Ref. 32 is induced by dislocation glide. The explicit strain field found in this latter work can be employed to calculate accurately the point-defect flux into a general grain-boundary geometry, in order to account also for climb in this type of simulation.

ACKNOWLEDGMENTS

This work was initiated while D.M. was a post-doctoral fellow at SRMP, CEA-Saclay in the framework of the French SMIRN (Simulation of Metal Irradiated in Nuclear Reactor) research program, the support of which is gratefully acknowledged. Partial support of the Russell Berrie Nanotechnology Institute is gratefully acknowledged. D.M.'s work at the Technion is supported in part by a Fine Fellowship. The authors are deeply thankful to Eugen Rabkin, Emmanuel Clouet, and Alain Barbu for fruitful discussions and advice. G.M. thanks Motoyasu Kinoshita and the NXO Japanese program for pointing out fascinating examples of microstructural evolutions in nuclear fuel materials.

APPENDIX: THE CAPTURE RADII OF DISLOCATIONS IN A TWO-DISLOCATION STRUCTURE

According to the isotropic elasticity theory, the strain field around a straight edge dislocation line in the positive z direction and a Burgers vector b in the positive x direction (Fig. 1) satisfies

$$\mathrm{tr}\left(\epsilon_{ij}^{\mathrm{dis}}\right) = -\frac{b}{2\pi}\frac{1-2\nu}{1-\nu}\frac{\sin\theta}{r}, \tag{A1}$$

and the nonzero components in the deviatoric strain tensor are

$$\begin{aligned}
\epsilon'^{\rm dis}_{xx} &= -\frac{b}{12\pi(1-\nu)}[(7-2\nu)\cos^2\theta + (1-2\nu)\sin^2\theta]\frac{\sin\theta}{r},\\
\epsilon'^{\rm dis}_{yy} &= \frac{b}{12\pi(1-\nu)}[(5+2\nu)\cos^2\theta - (1-2\nu)\sin^2\theta]\frac{\sin\theta}{r},\\
\epsilon'^{\rm dis}_{zz} &= \frac{b}{6\pi}\frac{1-2\nu}{1-\nu}\frac{\sin\theta}{r},\\
\epsilon'^{\rm dis}_{xy} &= \epsilon'^{\rm dis}_{yx} = \frac{b}{4\pi(1-\nu)}(\cos^2\theta - \sin^2\theta)\frac{\sin\theta}{r}.
\end{aligned} \tag{A2}$$

The contribution of a second dislocation, in a pair/dipole configuration, to the sink-strength calculation, is considered by taking its strain field at the position of the first dislocation. The contribution of the second dislocation in a pair structure ($\theta = 135^\circ$ or $\theta = -45^\circ$ and $r = \sqrt{2}h$) is

$$\begin{aligned}
{\rm tr}\left(\epsilon^{\rm dis}_{ij}\right) &= -\frac{b}{2\pi}\frac{1-2\nu}{1-\nu}\frac{\pm 1}{\sqrt{2}h},\\
\epsilon'^{\rm dis}_{xx} &= -\frac{b}{6\pi}\frac{2-\nu}{1-\nu}\frac{\pm 1}{\sqrt{2}h},\\
\epsilon'^{\rm dis}_{yy} &= \frac{b}{6\pi}\frac{1+\nu}{1-\nu}\frac{\pm 1}{\sqrt{2}h},\\
\epsilon'^{\rm dis}_{zz} &= \frac{b}{6\pi}\frac{1-2\nu}{1-\nu}\frac{\pm 1}{\sqrt{2}h},\\
\epsilon'^{\rm dis}_{xy} &= \epsilon'^{\rm dis}_{yx} = 0.
\end{aligned} \tag{A3}$$

The $\pm$ refers to the dislocation configuration in Figs. 1(a) and 1(b), respectively. If we sum both contributions, the nonzero strain field components in the vicinity of one of the dislocations is

$$\begin{aligned}
{\rm tr}\left(\epsilon^{\rm pair}_{ij}\right) &= -\frac{b}{2\pi}\frac{1-2\nu}{1-\nu}\left(\frac{\sin\theta}{r} \pm \frac{1}{\sqrt{2}h}\right),\\
\epsilon'^{\rm pair}_{xx} &= -\frac{b}{6\pi}\frac{2-\nu}{1-\nu}\left(\frac{\sin\theta}{r} \pm \frac{1}{\sqrt{2}h}\right),\\
\epsilon'^{\rm pair}_{yy} &= \frac{b}{6\pi}\frac{1+\nu}{1-\nu}\left(\frac{\sin\theta}{r} \pm \frac{1}{\sqrt{2}h}\right),\\
\epsilon'^{\rm pair}_{zz} &= \frac{b}{6\pi}\frac{1-2\nu}{1-\nu}\left(\frac{\sin\theta}{r} \pm \frac{1}{\sqrt{2}h}\right).
\end{aligned} \tag{A4}$$

We replaced $\cos^2$ and $\sin^2$ by their mean value, as in the analysis of Bullough and Willis.[19] This strain field is substituted in Eq. (5) to yield the interaction energy of a dislocation with a point defect, in the presence of a dislocation pair,

$$\begin{aligned}
kT\psi(\mathbf{r}) = {} & K\Omega\frac{b}{2\pi}\frac{1-2\nu}{1-\nu}\left(\frac{\sin\theta}{r} \pm \frac{1}{\sqrt{2}h}\right)\epsilon^{\rm misfit}\\
& + \alpha^K\frac{b^2}{4\pi^2}\frac{(1-2\nu)^2}{(1-\nu)^2}\left(\frac{\sin^2\theta}{r^2} \pm \frac{2}{\sqrt{2}h}\frac{\sin\theta}{r} + \frac{1}{2h^2}\right)\\
& + \alpha^G\frac{b^2}{36\pi^2}\frac{(2-\nu)^2 + (1+\nu)^2 + (1-2\nu)^2}{(1-\nu)^2}\\
& \times\left(\frac{\sin^2\theta}{r^2} \pm \frac{2}{\sqrt{2}h}\frac{\sin\theta}{r} + \frac{1}{2h^2}\right).
\end{aligned} \tag{A5}$$

If we combine the spatial-independent terms and the first- and second-order terms in $\sin\theta/r$ on the right-hand side of Eq. (A5), we get an equation of the form of Eq. (19) with a structure dependent capture radius (the prefactor of $\sin\theta/r$),

$$\begin{aligned}
R(h) = {} & \frac{K\Omega}{kT}\frac{b}{2\pi}\frac{1-2\nu}{1-\nu}\epsilon^{\rm misfit} \pm \frac{\alpha^K}{kT}\frac{b^2}{4\pi^2}\frac{(1-2\nu)^2}{(1-\nu)^2}\frac{2}{\sqrt{2}h}\\
& \pm\frac{\alpha^G}{kT}\frac{b^2}{6\pi^2}\frac{\nu^2-\nu+1}{(1-\nu)^2}\frac{2}{\sqrt{2}h}.
\end{aligned} \tag{A6}$$

The first term on the right-hand side is the capture radius of an isolated dislocation R_0 [Eq. (9)]. Equation (A6) can then be rewritten with R_0,

$$\begin{aligned}
R(h) = {} & R_0 \pm R_0\frac{\alpha^K}{K\Omega\epsilon^{\rm misfit}}\frac{1}{2\pi}\frac{1-2\nu}{1-\nu}\sqrt{2}\frac{b}{h}\\
& \pm R_0\frac{\alpha^G}{K\Omega\epsilon^{\rm misfit}}\frac{1}{3\pi}\frac{\nu^2-\nu+1}{(1-\nu)(1-2\nu)}\sqrt{2}\frac{b}{h},
\end{aligned} \tag{A7}$$

which leads to the interaction energy in Eq. (24) and the expression for $\kappa_{\rm pair}$ in Eq. (25).

In a similar fashion, the strain field about an isolated dislocation in a dipole structure is

$$\begin{aligned}
{\rm tr}\left(\epsilon^{\rm dipole}_{ij}\right) &= -\frac{b}{2\pi}\frac{1-2\nu}{1-\nu}\left(\frac{\sin\theta}{r} \pm \frac{1}{h}\right),\\
\epsilon'^{\rm dipole}_{xx} &= -\frac{b}{6\pi}\frac{2-\nu}{1-\nu}\frac{\sin\theta}{r} \mp \frac{b}{12\pi}\frac{1-2\nu}{1-\nu}\frac{1}{h},\\
\epsilon'^{\rm dipole}_{yy} &= -\frac{b}{6\pi}\frac{1+\nu}{1-\nu}\frac{\sin\theta}{r} \mp \frac{b}{12\pi}\frac{1-2\nu}{1-\nu}\frac{1}{h},\\
\epsilon'^{\rm dipole}_{zz} &= \frac{b}{6\pi}\frac{1-2\nu}{1-\nu}\left(\frac{\sin\theta}{r} \pm \frac{1}{h}\right).\\
\epsilon'^{\rm dipole}_{xy} &= \epsilon'^{\rm dipole}_{yx} = \mp\frac{b}{4\pi}\frac{1}{1-\nu}\frac{1}{h}.
\end{aligned} \tag{A8}$$

The $\pm$ sign refers to interstitial and vacancy dipoles, respectively. This strain field is employed to find the capture radius in Eqs. (26) and (27).

[1] G. S. Was, *Fundamentals of Radiation Materials Science* (Springer-Verlag, Berlin, 2007).
[2] M. Griffiths, J. Nucl. Mater. **159**, 190 (1988).
[3] F. A. Garner, J. Nucl. Mater. **205**, 98 (1993).
[4] D. O. Northwood, J. Nucl. Mater. **316**, 64 (1977).
[5] P. J. Maziasz, J. Nucl. Mater. **191-194**, 701 (1992).
[6] S. J. Zinkle, P. J. Maziasz, and R. E. Stoller, J. Nucl. Mater. **206**, 266 (1993).
[7] R. G. Vardiman, J. Appl. Phys. **71**, 5386 (1992).
[8] M. Kinoshita (private communication).
[9] W. G. Wolfer, J. Nucl. Mater. **90**, 175 (1980).
[10] P. Valentin and G. Martin, Philos. Mag. A **46**, 971 (1982).

[11]W. G. Wolfer and B. B. Glasgow, Acta Metall. **33**, 1997 (1985).
[12]C. H. Woo, J. Nucl. Mater. **80**, 132 (1979).
[13]V. I. Dubinko, A. S. Abyzov, and A. A. Turkin, J. Nucl. Mater. **336**, 11 (2005).
[14]W. G. Wolfer, J. Comput.-Aided Mol. Des. **14**, 403 (2007).
[15]J. P. Hirth and J. Lothe, *Theory of Dislocations* (McGraw-Hill, New York, 1968).
[16]J. D. Eshelby, Proc. R Soc. London, Ser. A **241**, 376 (1957).
[17]E. Kröner, Arch. Ration. Mech. Anal. **4**, 273 (1959).
[18]D. J. Bacon, D. M. Barnett, and R. O. Scattergood, Prog. Mater. Sci. **23**, 51 (1980).
[19]R. Bullough and J. R. Willis, Philos. Mag. **31**, 855 (1975).
[20]P. T. Heald and M. V. Speight, Acta Metall. **23**, 1389 (1975).
[21]I. G. Margvelashvili and Z. K. Saralidze, Sov. Phys. Solid State **15**, 1774 (1974).
[22]D. Mordehai, E. Clouet, M. C. Fivel, and M. Verdier, Philos. Mag. **88**, 898 (2008).
[23]G. Martin, Phys. Status Solidi B **172**, 121 (1992).
[24]J. Bardeen and C. Herring, in *Imperfections in Nearly Perfect Crystals*, edited by W. Shockley, J. H. Hollomon, R. Maurer, and F. Seitz (Wiley, New York, 1952), pp. 261–288.
[25]N. V. Doan and G. Martin, Phys. Rev. B **67**, 134107 (2003).
[26]M. H. Mathon, A. Barbu, F. Dunstetter, F. Maury, N. Lorenzelli, and C. H. de Novion, J. Nucl. Mater. **245**, 224 (1997).
[27]J. D. Torre, J-L. Bocquet, N. V. Doan, E. Adam, and A. Barbu, Philos. Mag. **85**, 549 (2005).
[28]M. C. Fivel, T. J. Gosling, and G. R. Canova, Modell. Simul. Mater. Sci. Eng. **4**, 581 (1996).
[29]D. Mordehai, E. Clouet, M. C. Fivel, and M. Verdier, IOP Conf. Ser.: Mater. Sci. Eng. **3**, 012001 (2009).
[30]R. E. Williford, C. H. Henager Jr., and J. P. Hirth, Acta Mater. **44**, 763 (1996).
[31]A. Kuper, H. Letaw Jr., L. Slifkin, E. Sonder, and C. T. Tomizuka, Phys. Rev. **96**, 1224(E) (1954).
[32]P. Moretti, M.-Carmen Miguel, and S. Zapperi, Phys. Rev. B **72**, 014505 (2005).